9-11-2013

A Review of Micro-Contact Physics for Microelectromechanical Systems (MEMS) Metal Contact Switches

Benjamin F. Toller
Air Force Institute of Technology

Ronald A. Coutu Jr.
Marquette University, ronald.coutu@marquette.edu

John W. McBride
Engineering Sciences University of Southampton

A review of micro-contact physics for microelectromechanical systems (MEMS) metal contact switches

Benjamin F. Toller
Air Force Institute of Technology, WPAFB, OH,

Ronald A. Coutu, Jr.
Air Force Institute of Technology, WPAFB, OH,

John W. McBride
Engineering Sciences University of Southampton Southampton, UK

Abstract

Innovations in relevant micro-contact areas are highlighted, these include, design, contact resistance modeling, contact materials, performance and reliability. For each area the basic theory and relevant innovations are explored. A brief comparison of actuation methods is provided to show why electrostatic actuation is most commonly used by radio frequency microelectromechanical systems designers. An examination of the important characteristics of the contact interface such as modeling and material choice is discussed. Micro-contact resistance models based on plastic, elastic-plastic and elastic deformations are reviewed. Much of the modeling

for metal contact micro-switches centers around contact area and surface roughness. Surface roughness and its effect on contact area is stressed when considering micro-contact resistance modeling. Finite element models and various approaches for describing surface roughness are compared. Different contact materials to include gold, gold alloys, carbon nanotubes, composite gold-carbon nanotubes, ruthenium, ruthenium oxide, as well as tungsten have been shown to enhance contact performance and reliability with distinct trade offs for each. Finally, a review of physical and electrical failure modes witnessed by researchers are detailed and examined.

1. Introduction

Low current micro-electrical contacts have a range of existing and potential applications. In microelectromechanical systems (MEMS) applications devices are normally referred to as a MEMS relay or MEMS switch, where a low force actuator is used to switch the micro-contact surfaces. In this review, the focus is on low power applications with both dc and ac signals. A particular emphasis is provided on the application to megahertz and gigahertz, radio frequency (RF) systems. RF MEMS switches can be used in mobile phones and other communication devices.[1] Often, micro-switches are used in phase shifters, impedance tuners and filters. Phase shifters, impedance tuners and filters are control circuits found in many communication, radar and measurement systems.[2] MEMS switches offer much lower power consumption, much better isolation, and lower insertion loss compared to conventional field-effect transistor and PIN diode switches, however, MEMS switch reliability is a major area for improvement for large-volume commercial applications.[3] The integrated circuit community is struggling to develop the future generations of ultralow-power digital integrated circuits and is beginning to examine micro-switches.[4] Low power consumption, isolation and reduced insertion loss are achieved by the mechanical actuation of the switch which physically opens or closes the circuit.

To enhance reliability, circuit designers need simple and accurate behavioral models of embedded switches in CAD tools to enable system-level simulations.[5] The MEMS literature indicates that varying the type of electrical load during testing reveals the physical limitation for micro-switches.[6] Rebeiz states that a good assumption for failure of the micro-switch is assumed to be when the contact resistance becomes greater than 5 Ω, which results in an insertion loss of –0.5 dB.[1] According to Rebeiz, the primary cause of micro-switch failure is due to plastic deformation in the contact interface such as 'damage, pitting, and hardening of the metal contact area [which] is a result of the impact forces between the top and bottom metal contacts'.[1] The description relates closely to 'cold' switching mechanical failure. 'Cold' switching is generally known to be actuating the switch repeatedly without applying RF or dc power during actuations, leading to micro-switch failures such as mechanical structural fatigue, memory effect and contact stiction.[6] In 'hot' switching, contributors to early micro-switch failure include 'material transfer high current density in the contact region and localized high-temperature spots'.[1]

2. Commonly used MEMS designs

In terms of design, the most common form of MEMS switch actuation is electrostatic in either a series or shunt configuration.[1,7] Electrostatic actuation offers the advantage of almost no power loss when the micro-switch is open.[1] By applying positive voltage to the actuation electrode, the grounded cantilever beam mechanically actuates and completes the signal path when the switch is closes. To open the switch, the applied voltage is removed. This allows the mechanical restoring force of the beam to become dominant over the electrostatic force and physically open the connection once contact adhesion is overcome. The electrostatic force is derived by treating the beam and actuation electrode as a parallel plate capacitor. When the beam width is w, the length of the pull down electrode is L, ε_0 is the permittivity of free space, g is the gap between the beam and the electrode, and then the given capacitance is:[8]

$$C = \frac{\varepsilon_0 A}{g} = \frac{\varepsilon_0 L w}{g}. \tag{1}$$

It then follows that the electrostatic force applied to the beam is:[8]

$$F_e = \frac{1}{2}V^2 \frac{dC(g)}{dg} = -\frac{1}{2}\frac{\varepsilon_0 L w V^2}{g^2}. \tag{2}$$

The linear mechanical spring restoring force is represented by Hooke's Law:

$$F_s = -kd = -k(g_0 - g) \tag{3}$$

where d is beam deflection, k is the spring constant and $(g_0 - g)$ is beam deflection from an initial gap distance g_0. Equating electrostatic force (2) and mechanical restoring force (3) results in:

$$\frac{1}{2}\frac{\varepsilon_0 L w V^2}{g^2} = k(g_0 - g). \tag{4}$$

From equation (4) the pull-in distance (i.e. $g = g_0/3$) and pull-in voltage are then solved for by finding the maximum value of (4) resulting in:

$$V_p = \sqrt{\frac{8}{27}\frac{k g_0^3}{\varepsilon_0 L w}}. \tag{5}$$

The pull-in distance and pull-in voltage is the point where the electrostatic force overcomes the beam's restoring force and the micro-switch closes by 'snapping down'. In RF MEMS, the series configuration is commonly used to pass signals along a signal path when the micro-switch is actuated while the shunt configuration is commonly used to short RF signals to a ground line.[1] Typically, shunt configuration MEMS switches are capacitive type for RF switching versus metal-to-metal contact type switches.[1]

Other forms of MEMS switch actuation mechanisms include: electrothermal, magnetic, and piezoelectric.[9–11] Electrothermal and magnetic actuation both offer the advantages of low control voltages and high contact force but draw high current and dissipate significant levels of power when actuated.[12] Both actuation mechanisms

have the advantage of being bi-directional and the disadvantages of slow actuation as well as quiescent power loss. Hysteresis is another disadvantage of magnetically actuated micro-switches. Piezoelectric actuation can provide fast actuation speeds but due to the different layers of material that comprise a piezoelectric material, there is a parasitic thermal actuation caused by a differential thermal expansion of the different layers. Piezoelectric actuation has a disadvantage of 'short throw' or small movement based on the number of stacked layers. Given the low power loss, low insertion loss and high isolation when open, electrostatic actuation is typically the most commonly used actuation method of RF MEMS engineers.

Micro-switch design considerations are normally focused on improving the micro-switch performance through mechanical design innovation not by improving micro-contact interfaces. From increasing contact force to reducing actuation voltage and decreasing switching time, all aspects of performance generally focus on beam geometry. Sometimes this is referred to as 'engineering away' the performance shortfalls of the micro-electrical contacts. The remainder of this paper focuses on micro-contact physics and phenomena that are relevant for MEMS metal contact switch design, performance and reliability.

3. Micro-contact resistance modeling

For dc micro-switches, resistance modeling requires knowledge of the surface of the two contact materials as well as their material properties. Though surface roughness and contamination can have a major impact on micro-contact resistance, they are not initially considered here and will be discussed later. Holm first identifies this in his example of contact resistance using two cylinders in contact at their bases.[13] Despite the surfaces of the cylinder bases appearing similar, they are actually very different. When two surfaces meet, and because no surface is perfectly smooth, asperity peaks or 'a-spots', from each surface meet at the interface and form contact areas. Asperities have been described as 'small cold welds providing the only conducting paths for the transfer of electrical current'.[7] The convergence and subsequent spreading of the electrical current through conducting a-spots is known as constriction resistance or commonly contact resistance.[13] For comparison, if two bulk material regions are continuous (not contiguous), with no conducting a-spots, then the resistance is called bulk resistance and calculated using $\frac{\rho l}{A}$ where, ρ is the resistivity, l is the length and A is the cross-sectional area of the conducting material. Figure 1 shows a graphical representation of apparent contact area, contacting a-spots, and the effective radius of the actual conducting area.[14]
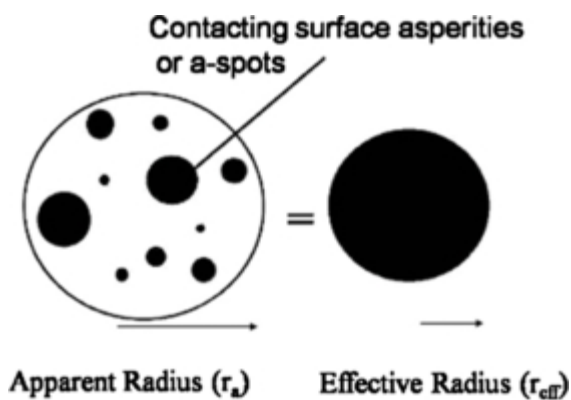

Figure 1. A-spots as an effective radius.[14]

The effective contact area is used for making simplified contact resistance calculations and provides an upper bound when estimating micro-contact resistance.[15] Holm also investigated contact resistance changes due to plastic and elastic deformation of a-spots; which greatly affects the interface of the contact areas.[13]

Majumder *et al* modeled micro-contact resistance with three steps.[15] First, determine the contact force, as a function of applied gate voltage, available from the mechanical design of the electrostatically actuated micro-switch. Second, determine the effective contact area at the interface as a function of contact force.[15] Finally, determine the contact resistance as a function of the distribution and sizes of the contact areas. Majumder *et al* like Holm, also noted that the surface profile of the contact interface is sensitive to plastic and elastic deformation. He also investigated ballistic electron transport using Sharvin's equation.[15]

Elastic modeling is accurate for extremely low values of contact force (tens of µN's) where surface asperities retain their physical forms after the contact force is removed. Elastic-plastic deformation occurs at the boundary between the permanent plastic deformation and the temporary elastic deformation. Under plastic deformation, permanent surface change occurs by the displacement of atoms in asperity peaks whereas neighboring atoms are retained under elastic deformation.[16]

Single asperity contact area and force under elastic deformation are given by:[17]

$$A = \pi R \alpha \qquad (6)$$

$$A = \pi R \alpha$$

where *A* is contact area, *R* is asperity peak radius of curvature, and α is asperity vertical deformation and

$$F_{cE} = \tfrac{4}{3} E' \alpha \sqrt{R\alpha} \qquad (7)$$

$$F_{cE} = \frac{4}{3} E' \alpha \sqrt{R\alpha}$$

where *E'* is the effective Hertzian modulus derived from:

$$\frac{1}{E'} = \frac{1 - v_1^2}{E_1} + \frac{1 - v_2^2}{E_2} \qquad (8)$$

$$\frac{1}{E'} = \frac{1 - v_1^2}{E_1} + \frac{1 - v_2^2}{E_2}$$

where E_1 as the elastic modulus for contact one, v_1 is Poisson's ratio for contact one, E_2 as the elastic modulus for contact two, v_2 is Poisson's ratio for contact two.[7,13] For circular areas, (6) and (7) are related to the contact area radius using Hertz's model:[13]

$$r_{\text{eff}} = \sqrt[3]{\frac{3F_{cE}R}{4E'}}. \qquad (9)$$

$$r_{\text{eff}} = \sqrt[3]{\frac{3F_{cE}R}{4E'}}.$$

To account for the asperity contact area and force under plastic deformation, the well known model from Abbot and Firestone that assumes sufficiently large contact pressure and no material creep is used.[18] Single asperity contact area and contact force are defined using (10) and (11):[18]

$$A = 2\pi R\alpha \qquad (10)$$

$$A = 2\pi R\alpha$$

$$F_{cP} = HA \qquad (11)$$

$$F_{cP} = HA$$

where H is the Meyer hardness of the softer material,[18] A is contact area, R is asperity peak radius of curvature, and α is asperity vertical deformation.[18] The effective contact area radius for circular areas is then related to contact force by:

$$r_{\text{eff}} = \sqrt{\frac{F_{cP}}{H\pi}}. \qquad (12)$$

$$r_{\text{eff}} = \sqrt[3]{\frac{F_{cP}}{H\pi}}.$$

While plastic and elastic definitions are helpful, a thorough description of deformation cannot be provided without considering the elastic-plastic transition between the two kinds of deformation. Elastic-plastic material deformation asperity contact area and force are given as:[17]

$$A = \pi R\alpha \left(2 - \frac{\alpha_c}{\alpha}\right) \qquad (13)$$

$$A = \pi R\alpha \left(2 - \frac{\alpha_c}{\alpha}\right)$$

$$F_{cEP} = K_H A \qquad (14)$$

$$F_{cEP} = K_H A$$

where α_c is the critical vertical deformation and K_Y is the yield coefficient where elastic-plastic behavior begins.[17] Effective contact area radius is given by:[17]

$$r_{\text{eff}} = \sqrt{\frac{F_{cEP}}{H\pi \left[1.062 + 0.354 \left(\frac{2}{3}K_Y - 3\left(\frac{\alpha_c}{\alpha}\right)\right)\right]}} \qquad (15)$$

$$r_{\text{eff}} = \sqrt{\frac{F_{cEP}}{H\pi \left[1.062 + 0.354 \left(\frac{2}{3} K_Y - 3\left(\frac{\alpha_c}{\alpha}\right)\right)\right]}}$$

Equations (9), (10), and (15) provide the key relationships between contact force and effective conducting area. It is important to note that contact force directly influences the effective conducting area and will also impact contact resistance by default.

Based on the size of the effective conducting area and how it compares with the mean free path of an electron, current flow is described as being ballistic, quasi-ballistic, or diffusive.[19]

Previously, Wexler derived a Gamma function interpolation as a function K, or the Knudsen number, for electron conduction when transitioning between ballistic and diffusive electron transport regions.[20] The Knuden number is a dimensionless quantity defined as the ratio between mean free path length (in this case electron mean free path or l_B) to a reprentative length scale (in this case the radius of a conducting area or l).[20] Wexler's Gamma function, shown in figure 2, depicts complete diffusive transport ($\Gamma w \approx 1$) for small Knudsen numbers ($K < 0.02$) and approximately 68.3% ballistic transport for large Knudesn numbers ($K > 7.0$). Majumder $et\ al$ used Wexler's Gamma function and developed the following micro-contact resistance model:

$$R_w = R_S + \Gamma w(K) R_c \qquad (16)$$

$$R_\omega = R_S + \Gamma w(K) R_c$$

where R_w is the Wexler-based contact resistance, $\Gamma w(K)$ is the Wexler Gamma function (shown in figure 2) for transitioning between ballistic and diffusive transport regions, R_S is the Sharvin resistance based on ballistic electron transport and R_c is the Holm constriction resistance based on plastic deformation and diffusive electron transport.[15] The semi-classical approximation for resistance when electrons exhibit ballistic transport behavior is the Sharvin resistance formula (17).[15]

$$R_S = \frac{4\rho K}{3\pi r_{\text{eff}}}. \qquad (17)$$

$$R_S = \frac{4\rho K}{3\pi r_{\text{eff}}}$$
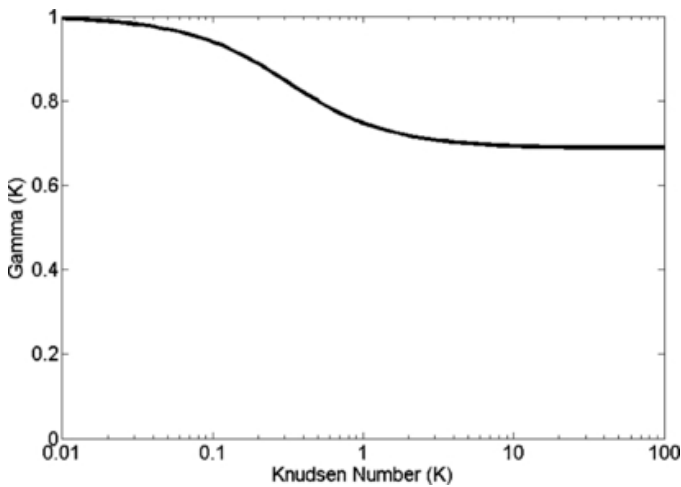
Figure 2. A plot of Wexler's Gamma function as a function of Knudsen.

Majumder $et\ al$'s original model was improved by Coutu $et\ al$ when elastic deformation and diffusive electron transport as well as elastic deformation and ballistic electron transport were considered by (18).[19]

$$R_{\text{WE}} = R_{\text{SBE}} + \Gamma m(K) R_{c\text{DE}} \qquad (18)$$

$$R_{\text{WE}} = R_{\text{SBE}} + \Gamma m(K) R_{c\text{DE}}$$

where, R_{WE} is the Wexler-based contact resistance for elastic material deformation, R_{SBE} is the Sharvin (ballistic, elastic) resistance term and Rc_{DE} is the Holm (diffusive, elastic) resistance term.[19] In this new model, $\Gamma m(K)$ is not Wexler's slowly varying Gamma function of unity order but has been replaced by Mikrajuddin *et al*'s well behaved Gamma function that describes complete diffusive (when $K < 0.02$, $\Gamma m \approx 1$), quasi-ballistic (when $K \approx 1$) and complete ballistic transport (when $K > 20$, $\Gamma m \approx 0$):

$$\Gamma m(K) \approx \frac{2}{\pi} \int_0^\infty e^{-Kx} \text{Sinc}(x)\, dx. \qquad (19)$$

$$\Gamma m(K) \approx \frac{2}{\pi} \int_0^\infty e^{-Kx} \text{Sinc}(x) dx.$$

Figure 3 shows a plot of Mikrajuddin *et al*'s derived gamma function which describes electron flow as a function of the Knudsen number or K.[21] The significance of Mikrajuddin *et al*'s result is that it describes situations for complete diffusive electron transport or complete ballistic electron transport whereas Wexler's original derivation included all higher order effects (e.g. electron spin, electron distribution, etc) resulting in higher than expected contact resistance estimates for contacts operating entirely in the ballistic region (e.g. nano-sized contacts).[21]
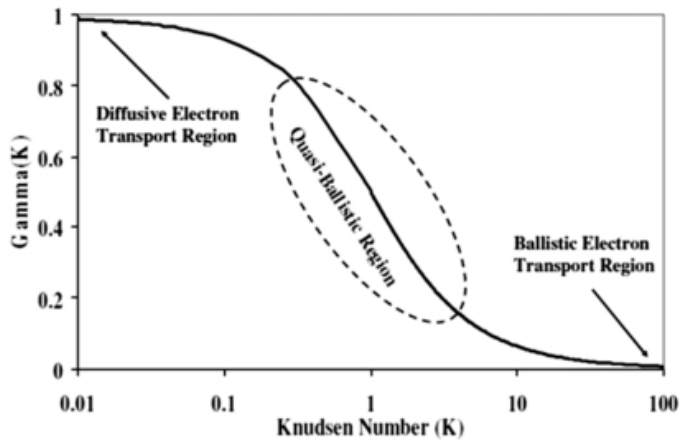
Figure 3. A plot of Mikrajuddin *et al*'s derived Gamma function with ballistic, quasi-ballistic and diffusive electron transport regions highlighted.[19]

Coutu *et al* further developed this model by considering elastic-plastic deformation in the micro-contact resistance equation for ballistic and diffusive electron transport, shown in equations (20) and (21), respectively[19]

$$R_{cBEP} = \frac{4\rho K}{3\pi} \sqrt{\frac{H\pi \left[1.062 + 0.354 \left(\frac{2}{3}K_Y - 3\left(\frac{\alpha_c}{\alpha}\right)\right)\right]}{F_{cEP}}} \qquad (20)$$

$$R_{cBEP} = \frac{4\rho K}{3\pi} \sqrt{\frac{H\pi \left[1.062 + 0.354 \left(\frac{2}{3}K_Y - 3\left(\frac{\alpha_c}{\alpha}\right)\right)\right]}{F_{cEP}}}$$

$$R_{cDEP} = \frac{\rho}{2}\sqrt{\frac{H\pi\left[1.062 + 0.354\left(\frac{2}{3}K_Y - 3\left(\frac{\alpha_c}{\alpha}\right)\right)\right]}{F_{cEP}}}. \quad (21)$$

With (20) and (21) the new model for micro-contact resistance that accounts for elastic-plastic contact deformation is provided as (22):[19]

$$R_{WEP} = R_{cBEP} + \Gamma(K)R_{cDEP}. \quad (22)$$

The above micro-contact models assume electrical current flow is between two contiguous bulk conducting materials and the current flows through conducting a-spots or constrictions and do not explicitly account for quantum effects or the spreading resistance resulting from thin film micro-contacts. The spreading resistance, developed on either side of a thin film constriction, inherently affects micro-contact resistance and will be discussed later.

To model spreading resistance, Karmalkar *et al* developed a simple closed-form model to predict accurate and complex calculations of circular and rectangular contact spreading resistances.[22] The method was to solve the three dimensional Laplace equation

$$\nabla^2\psi = 0 \quad (23)$$

subject to the appropriate boundary conditions in several iterations to consider changing geometries. Holm, by contrast, represented spreading resistance as a 5% increase in constriction resistance.[13] By interpolating the results of the different geometric solutions, the resistance average was calculated.[22] Experimental tests revealed close (within 2%) agreement with standard numerical analysis software. Their study found that the developed model accurately predicts all the trends of resistance, to include a significant variation as a function of the smaller electrode location, dependence on the electrode separation-to-width ratio, and saturation with increase in the larger electrode area for both equipotential and uniform current density boundary conditions.[22]

When considering micro-contacts, surface contamination has severe negative impacts for electrical contacts by physically separating the conductive electrode surfaces.[23] Based on thickness and composition, the adsorbed contaminants can increase contact resistance by orders of magnitude.[23] When left exposed to the ambient lab air, device surfaces can be covered with various contaminants which will affect conductivity.[24] This concept was experimentally verified by Lumbantobing *et al* where during cyclical contact loading, electrical contact resistance was erratic due to the strong dependence of contact resistance on an insulating thin film at the contact interface.[25] Lumbantobing *et al* also experienced reduced electrical contact resistance on contacts with native oxides during cyclic contact loading and attributed the reduced resistance to the local rupture of the film, resulting in asperity nanocontacts that reduced the resistance.[25] They also found that the nearly uniform

thickness of the native oxide film predicted in their experiment illustrated the durability and robustness of oxide thin film under the tested loading conditions.

Timsit explored the effect of constriction resistance on thin film contacts. He postulated that the spreading resistance of an asperity in a thin film will be drastically different than of an asperity in bulk material due to the different boundary conditions.[26] His study confirmed that the contact resistance for a contact with two identical films can be immediately calculated as twice the spreading resistance.[26] Also, the constriction resistance between two films of the same thickness L in contact over a constriction of radius a deviates greatly from the classical expression $p/2a$ for two contacting bulk solids wherever $a/L \geq 0.02$.[26] A counter-intuitive discovery was shown revealing that spreading resistance in a radially-conducting film initially decreases with decreasing film thickness.[26] This is counter-intuitive because the resistance of a solid conductor increases with decreasing thickness.[26] Timsit's approach was very similar to those published by Norberg *et al* whereby contact resistance in thin films was approximated by empirical modifications of Holm's classical relation:

$$R_c = \frac{\rho}{2a} \qquad\qquad (24)$$

$$R_c = \frac{\rho}{2\alpha}$$

where ρ is the resistivity of the conducting material and a is the radius of the constriction.[13,27] However, Norberg *et al* used finite element modeling (FEM) to approximate constriction resistance for complex geometries and neither researchers considered the effects ballistic electron transport and the Sharvin effect.[26,27]

In another work, Timsit examined the major electrical conduction mechanisms through small constrictions and concluded that the onset of the Sharvin resistance, which stems from ballistic electronic motion in a constriction, eventually invalidates the basic assumptions of classical electrical contact theory.[28] This finding validates Coutu *et al*'s use of Mikrajuddin *et al*'s derived gamma function. Timsit reported through the use of a simple a-spot model and quantum mechanics that the cooling of a small a-spot due to heat loss by the surrounding electrically-insulating films is not sufficiently large enough to have an impact or account for the breakdown of classical theory. The conjecture is proposed that for metal atomic scale constrictions, a single atom corresponds to a single conductance channel which implies that the conductance would not decrease smoothly as the mechanical contact load is decreased.[28] Rather, the conductance will drop in well defined quantized steps since the number of contacting atoms is decreased by discrete units of one or a few at a time.[28,29]

To examine contact resistance models based on thin films, Sawada *et al* performed a current density analysis of thin film effects in the contact area on a LED wafer.[30] By using a unique setup with an indium bump to bond to a gallium phosphorous wafer, the team was able to examine and image current flow through a contact. Imaging was possible because the current flow caused optical emission in the wafer. The images and results showed that the current flow in the contact was located primarily around the perimeter of the contact. The use of imaging enabled greater insight in determining actual micro-contact area. The research showed that classical theory for contact resistance was sufficient, provided the conducting film was relatively thick (200 μm).[30] In comparison with Timsit's model for the constriction resistance of thin films, the results were in agreement. However, when the film thickness was 50 μm or less, the value of the contact resistance was greater than the bounds of the classical theory. The thin film work of Timsit, Norberg *et al* and Sawada *et al* collectively provided necessary insight for future micro-contacts studies since the thin films they studied were similar to films routinely used to fabricate electrical contacts for MEMS switches.

Assumptions about asperity size and quantity greatly impact contact resistance calculations. While most contact resistance models consider only single 'small' constrictions, the typical rough surface may include many small contacts of varying sizes. However, quantum effects may be present with sufficiently small contacts. To investigate the quantum and size dependent contact mechanisms of the asperity sizes on typical surfaces, Jackson *et al* examined the effect of scale dependent mechanical and electrical properties on electrical contact resistance between rough surfaces.[31] Beginning with classical contact mechanics, they used established multi-scale models for perfectly elastic and elastic-plastic contacts for the purpose of predicting electrical contact resistance between surfaces with multiple scales of roughness. They then examined scale dependent strength of the materials tin (Sn) and gold (Au) and found that the yield strength varies by over two orders of magnitude as the contact diameter changes. Lastly, using an iterative multi-scale sinusoidal method to calculate the average radius of a contact at given scales, an analytical model of electrical contact resistance was developed.

Unlike Timsit, Poulain *et al* examined quantized conductance experimentally with micro-contacts test apparatus for breaking contact in such a way that the dimensions of the conducting members of the micro-contact were much smaller than the mean free path of an electron.[32] The team found that by using a micro-switch and a nanoindentor, they were able to witness quantized conductance plateaus before separation of the two contact members. The conditions for observing the quantized conduction phenomena are an extremely low switch opening speed and a current limitation near 150 μA.[32] Upper and lower micro-contacts made of Au as well as micro-contacts made of Ru–Ru were tested. Independent of the contact material, quantized conductance behavior was witnessed. The plateaus were consistent with theoretical predictions for quantum ballistic transport in atomic-sized contacts. The work showed that a metallic bridge formed during contact separation, in the last stage of contact break, and consisted of only a few atoms similar to a nanowire or waveguide thus revealing the wave character of the electrons.[32] The team observed that reproducibility of the results was difficult due to the fact that the elongation of the atomic-sized bridge is difficult to control and was strongly related to atomic arrangements.[32]

While dealing with the quantum theory to describe current flow through nano-scale asperities continues to be explored, some researchers have developed methods to simulate electrical contact resistance of ohmic switches with finite element modeling (FEM). Pennec *et al* examined the impact of surface roughness on the electrical contact resistance under low actuation forces (from a few tens of μN's to 10 mN).[33] An important aspect of their work was to clearly define the surface roughness of the contact. Common practice is to take the average radius of curvature of the asperities which is determined by a measurement of the surface profile.[34] The drawback to this common method is that the determination of the average radius is subjective to the scale of the observation, and is also limited by the measurement resolution.[35–37] In order to clearly define the surface roughness of the contact, three methods were examined: statistical, fractal, and deterministic.[33] A statistical approach, based on a stochastic analysis, is limited to the resolution of the measuring instrument.[33] A fractal method, on the other hand, uses a random surface texture that is characterized by scale-independent fractal parameters.[33]

The deterministic approach is often chosen due to its closest representation of an actual surface.[33,38] Deterministic methods capture discrete data points for real heights on the surface which avoids assumptions of the micro geometry of the a-spots.[33] Kogut states that even though there are several methods to model contacting rough surfaces, the most convenient one is the probabilistic approach developed by Greenwood and Williamson.[38,39] This approach replaces the two rough surfaces by a smooth surface in contact with an equivalent rough surface, replacing asperities with simple geometric shapes, and assuming a probability distribution for the asperity parameters.[40]

Using an AFM, surface topography of the contact bumps was measured and a low resolution mesh was generated in order to quickly determine the effective contact area under 100 μN of force.[33] By stepping up the

resolution for the effective contact area to the effective computation memory limits, Pennec *et al* were able to model a contact resistance in agreement with literature.[33] While their method did not take into account contaminant films, the results show that including the fine-scale details of the surface roughness must be taken into account when calculating contact resistance.[33] However, while AFMs can achieve 1 nm resolution of surfaces, the number of contact elements and definition of elastic-plastic materials in the model can prevent the calculations from succeeding due to computer memory limitations.[33] Conclusive evidence is given that reducing the sampling interval from 1 nm to 10 nm is sufficient for the calculation of electrical contact resistance.

Proponents of fractal models, Rezvanian *et al* believe that the random and multiscale nature of the surface roughness can be better described by fractal geometry.[7,41] Fractal based models have been developed by a number of researchers but lack considerations for elasticity.[42,43] Persson *et al* developed a novel fractal method which is not dependent on fractal roughness and is also not scale dependent like the Greenwood model.[44,45] The disadvantage is that this method is exclusive to fractal surfaces.[46]

Similar in nature, Jackson *et al* considered multi-scale roughness, or the description of the surface, to be sinusoids stacked into layers to represent the rough surface.[47] While quantitative discrepancies exist between the statistical methods and layered sinusoids, the team was able to show qualitative similarities for both elastic and elastic-plastic deformation.[47] In fact, until higher force loads are reached, the model is very much in agreement with standard methods.[47] At higher loads where the contact radius is large compared to the asperity tip radius, the models differ greatly.[47] This method of stacking sinusoids however is not limited to contact resistance but is also employed to model adhesion.[48] Where the classical approximation for area is a simplified model that typically bundles asperities into a few, the stacked sinusoids allow for a more practical representation of a multiscale surface.[48]

So far, it is apparent that the surface of the physically connecting electrodes is a key factor for the determination of electrical contact resistance. Modifications to the surface via a thin film from adsorbed contaminants from either ambient air or hermetic environments will greatly decrease the conductivity of the contact. To improve electrical conduction between contacts, Jackson *et al* have tried to reduce the contact resistance by applying an anisotropic conductive thin film.[49] These films are typically an epoxy that is doped with conductive metal particles.[49] While classical electrical resistance theory falls short for accurately predicting the contact resistance with an insulating thin film, a model is proposed by Jackson and Kogut to consider elastic-plastic behavior of the thin film and large deformations of the conductive particles.[49] While previous anisotropic conductive film models have under predicted electrical contact resistance, a conjecture was made that the difference may be accounted for by the quantum effect of electron tunneling that takes place through the energy barrier imposed by the thin film.[49] This 'tunneling' resistance is higher than the constriction resistance.[49] Using empirical models, mechanical and electrical material constants were held constant and the radius of the conductive particles in the film were varied.[49] The results revealed that particle size influenced contact resistance and that the larger radius provided a lower resistance.[49]

When it comes to micro-contact resistance modeling, contact material deformation and the effective contact area radius are the two primary considerations.[15] An assumption that individual a-spots are sufficiently close and that a single effective area model is typically made to determine specific electron transport regions by comparing the effective radius and mean free path of an electron.[19] As seen by area models to characterize the surface topology, describing the appropriate effective area for modeling is difficult. From the modeling of the surface using statistical, deterministic, or fractal means to the models of contact resistance based on all the deformation modes, the development of a thin film will widen the variance between simulated and actual results. Contact materials also have an integral role in determining the performance and reliability of micro-switches. Hardness as well as conductivity and other material properties influence the contact resistance. Gold (Au), palladium (Pd), and platinum (Pt) are commonly used.[50] Due to the fact that these materials are very soft

and wear easily, other materials such as nickel (Ni), ruthenium (Ru), ruthenium oxide (RuO$_2$) and combinations or alloys of materials have also been examined for their effectiveness at lengthening the lifecycle and the performance of micro-electrical contacts.[3,19,50–52]

4. Contact materials for performance and reliability

The earlier discussion of micro-contact resistance modeling showed how the material properties of the contact impact the contact resistance. The intrinsic properties of the materials chosen for the contact are important for increasing the lifecycle of the contact. For instance, due to its low electrical resistivity and low sensitivity to oxidation.[53] gold is widely employed as a contact material in MEMS.[54] In general, electrical contacts are desired to have low electrical conductivity, a high melting point, an appropriate hardness to avoid material transfer and chemical inertness to avoid oxidation.[55] As will be discussed in the failure modes and reliability section, material transfer can take place less easily with harder materials. Material hardness is an important property as the surface of the contact will change with actuations over time. As the surface changes, changes to contact resistance occur simultaneously. Alloys are often created in order to take advantage of material properties to try and minimize the effect of material transfer.[3] Yang *et al* showed Au–Ni alloy contacts resist material transfer better than Au–Au contacts.[3]

McGruer *et al* showed that ruthenium (Ru), platinum (Pt), and rhodium (Rh) contacts were susceptible to contamination and the contact resistance increased after a characteristic number of cycles, while gold alloys with a high gold percentage showed minimal contact resistance degradation under the same test conditions.[3,56] Similarly, Coutu *et al* showed that alloying gold with Pd or Pt extended the micro-switch lifetimes with a small increase in contact resistance.[19] Failure is typically defined as an increase in contact resistance beyond a given tolerance set by the circuit designer. Contact resistance tends to increase towards the end of a micro-switches lifetime.

As will be discussed later, frictional polymers are carbon based insulating films which develop over time and tend to increase contact resistance.[7] Despite carbon being a core component to frictional polymers, Yaglioglu *et al* examined the electrical contact properties of carbon nanotube (CNT) coated surfaces.[57] The high Young's modulus and potential for low resistance of CNTs makes them suitable candidates for micro-switch contacts. For instance, Au contacts with a substrate coated with tangled single-walled CNTs were shown to have a resistivity between 1×10^{-4} and 1.8×10^{-4} Ωm.[58] CNTs have been reported to have an elastic modulus of approximately 1 TPa, which is comparable to diamond's elastic modulus of 1.2 Tpa.[59] Yunus *et al* explored two contact pairs with CNT: Au to multiwall CNT (MWNTs), where one electrode is Au and the other is MWNTs, and Au to Au/MWNT composite, where the contact interface is Au–Au.[60] Figure 4 shows an SEM image of the Au–MWNT composite.
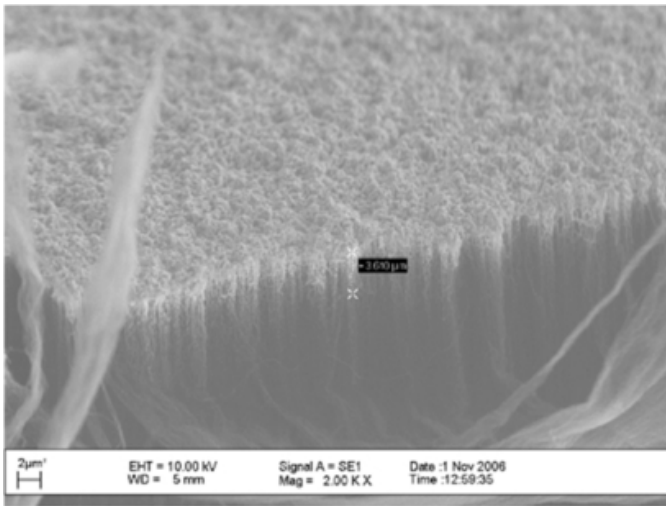
Figure 4. 2–4 µm of Au coating on MWNT. © 2009 IEEE. Reproduced with permission from.[60]

It was found that the Au–Au/MWCNT was the better performer than Au–MWCNT in terms of contact resistance.[60] While the MWCNTs did not improve contact resistance, the modulus of the lower contact was enhanced which could lead to greater reliability. The data, shown in figure 5, was collected with a nanoindentor apparatus which cycled for ten repeated operations with a maximum applied load of 1mN.[60] The hardness of each material is also dramatically different, approximately 1 TPa for CNT and 1 GPa for Au.[60] The CNT structure supporting the Au film acts to allow the Au film to deform elastically under the applied load. In this study, a hard Au coated steel ball is making contact with the softer Au/MWCNT surface. The latter surface deforms to the shape of the steel ball, increasing the apparent contact area. With the Au coated steel ball in contact with the MWCNT surface the conduction path is through the lateral connection of the vertically aligned CNTs; leading to a higher contact resistance. A disadvantage to the mechanical design of the switch was discovered to be excessive bouncing on closure; that is, the contact takes time to settle in the closed position.
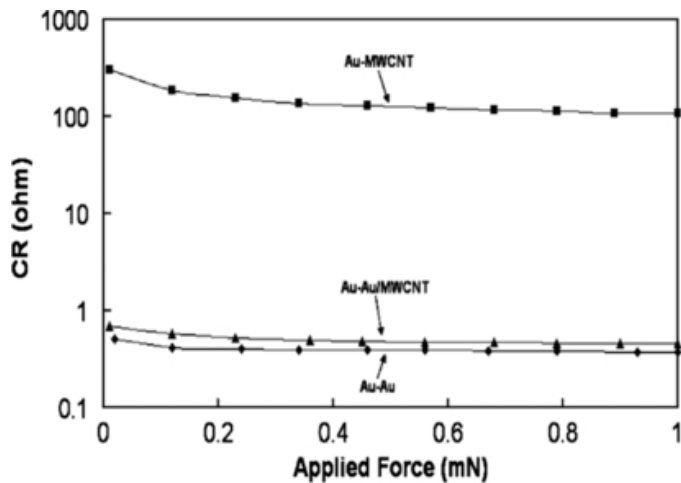
Figure 5. Comparison contact resistance (CR) of Au–MWCNT to Au–Au/MWCNT and Au–Au contacts. © 2009 IEEE. Reproduced with permission from.[60]

A study was conducted by Choi *et al* to explore the current density capability of a CNT array with an average CNT diameter of 1.2 nm, site density of 2CNT/µm, and the number of CNTs for devices with 1 µm channel width ranged from one to three.[61] It was reported that a high current density of 330 A cm^{-2} at 10 V bias was successfully transmitted through the contact without any noticeable degradation or failure.[61] A reliability test

with an input current of 1 mA showed repeatable and consistent contact characteristics over a million cycles of operation.[61]

It is reported in literature that the small contact area between CNT and a metal electrode makes electrical coupling between them extremely difficult.[62–65] An experiment was performed by Chai *et al* to verify if a graphite interfacial layer would increase the electrical contact to the CNTs.[62] Graphite was chosen due to its close material properties to the CNTs namely, metal-like resistivity and similar chemical bonding.[62] A common technique for carbon deposition to the CNT contact region is to use the electron beam inside of a scanning electron microscope (SEM) to induce carbon deposition.[62] The technique is reported to successfully form low resistance electrical contact to MWCNTs.[66,67] Chai's experiment validated that the graphitic carbon interfacial layer did reduce the contact resistance due to the increase in contact area to the CNT.[62]

In an example of engineering a contact for increased lifetime, Ke *et al* coated Au contacts with Ru to investigate placing harder materials with relatively low resistivity on top of softer materials with lower resistivity.[68] The contact resistance and life time of the Ru layered Au switch were compared to the common Au–Au micro-contact switches.[68] The switches demonstrated a life time enhancement of over ten times as measured in a non-hermetic environment as compared to pure, soft gold contacts.[68] On the other hand, alloying Au with other metals results in increased hardness, but also an increased resistivity.[69] Atomic-level simulations and experimental observations have shown that the separation of gold contacts leads to considerable material transfer from one side of the contact to the other.[70–72]

Broue *et al* characterized Au–Au, Au–Ru, and Ru–Ru (upper and lower contact materials respectively) ohmic contacts by examining the temperature of the contact in the on-state to determine its performance limitations.[51] For the Au–Au contact, the contact temperature was linear and stable but the fluctuated between 80 °C and 120 °C after the application of 40 mA.[51] This is agreeable with the reported maximum allowable current for gold contacts of 20 to 500 mA.[73] The published softening temperature for a gold contact is ~100 °C, which corresponds to a contact voltage of 70–80 mV for a contact near room temperature.[13] Comparatively, the published softening temperature for a ruthenium contact is ~430 °C, corresponding to a contact voltage of 200 mV for a contact near room temperature.[73] The Ru–Ru contact exhibited similar behavior in that it fluctuated about 400 °C after reaching a critical current level of 30 mA.[51] The contact with the best performance was the Au–Ru combination contact, where the contact temperature increased with the current level without reaching a maximum.[51] The experiment went as far as to apply 100 mA for all three combinations.[51] An explanation to the difference in performance was offered that the contact temperature of the Au–Ru contact is more stable because the softening temperature is theoretically not reached for the same contact current.[51]

In the interest of exploring the limitations of Ru, Fortini *et al* compared how asperity contacts form and separate in gold and ruthenium.[74] Their technique was to establish an appropriate interatomic potential in order to apply a molecular dynamics (MD) simulation, which is a powerful tool for studying adhesion, defect formation and deformation on the nano-scale level.[74] The MD technique enabled the team to understand the formation and separation of nanoscale asperity contacts by simulating the motion of the atoms.[75] The simulations showed that Ru was ductile at T = 600 K and more brittle at T = 300 K, where it separated by a combination of fracture and plasticity.[74] Gold exhibited ductile behavior at both T = 150 K and T = 300 K.[74,76] The difference in ductile/brittle behavior of the Au and Ru contacts was consistent with FEM calculations in literature.[77]

Other researchers have explored using tungsten (W) as the contact material. Tungsten was chosen for its hardness and resistance to mechanical stress and physical deformation.[78] Kam *et al* verified that W was beneficial for improved resistance to wear and micro-welding.[79] A disadvantage of W was its susceptibility to chemically react and form oxides on the surface.[78] It is reported that oxidation of exposed W electrode surfaces occurs if there is any ambient oxygen, which increases the rate of oxidation exponentially with increasing

temperature.[80] This was verified by Spencer *et al*, who studied the oxide layers as they became thicker with exposure times; they offered the theory that the exacerbated rate of oxidation was due to the widening of the oxygen diffusion path as the oxide gets thicker.[81] This thin film of oxide negatively impacts the contact resistance and requires higher contact loading to break through the film and obtain low resistance. The experiments of Chen *et al* show that W electrodes exhibit an undesirable increase in on-state resistance over the lifetime of the device.[78] The oxidation of W was sped up by the amount of current flowing through the contact. Energy losses in the form of heat increased the opportunity and rate of thermal oxidation. They offered two solutions to the oxidation problem of W electrodes: either use another material or minimize device exposure to oxygen with a wafer-level encapsulation process.[78,82]

Yamashita *et al* investigated the use of an anti-stiction coating for ohmic micro-contacts under low loads (0 to 70 μN).[83] The contacts were coated with thiophenol and 2-naphthalenethiol. The coatings successfully prevented the formation of the liquid meniscus, reduced the capillary force better than the bare Au surfaces, and reduced the van der Waals forces.[83] They also noted that increased surface roughness could prevent stiction exponentially by reducing the effective contact area.[83] Increasing surface roughness would trade performance in terms of lower contact resistance which relies on large effective area of contact for anti-stiction properties. With the coatings applied, contact resistance decreased after 16 μN but required at least 4 μN of contact force for current to begin to flow.[83] It was found in the study that the contact resistances of the samples deposited with a 100 nm-thick Au layer were slightly smaller than those with a 20 nm-thick Au layer despite the larger resistivity value for the thicker layer due to the relationship between surface roughness and resistivity.[83,84] An answer was offered by Yamashita *et al* that the contact area between the electrodes was larger for the thicker layer because the electrodes made contact with large crystal grains.[83] Consistent with literature and classical theory, the results showed that contact resistance decreased proportionally with increasing contact force for all samples.[83] Because of increased contact forces, the contact resistance drops with an increase in asperity deformation, which provides a greater contact area as the micro-geometry changes.[85,86]

As expressed earlier, increases in contact area decrease electrical contact resistance. One method to increase contact area was examined by Baek and Fearing using compliant nickel nanowire arrays.[87] The concept was to guarantee an approximate number of contact points for current to flow when the electrode surfaces mate instead of relying on rough approximations for asperity micro-geometry. Since the nanowires are compliant, the effective contact area would increase as contact force is increased overall decreasing contact resistance. The array was employed to achieve a minimum contact resistance of 73 mΩ for a contact area of 0.45 mm^2 using an array of compliant nickel nanowire.[87] The wires were fabricated by electrodeposition and porous filters in order to achieve a maximum aspect ratio of 300:1 (60 μm × 0.2 μm).[87]

Regarding the reduction electrical contact resistance for tin (Sn) contacts, Myers *et al* proposed a new contact design in order to lower contact resistance which is not limited to Sn.[88] The fundamental principle behind the concept was that when classical Hertzian surfaces make contact, the mechanical load is carried by asperities in the center of the contact while the electrical load is distributed by asperities along the outer rim of the contact. As oxides and other surface contaminants may appear, the team suggested designing contacts so that the outer rim asperities are the only asperities that would make contact thus bearing both the mechanical and electrical load. This approach would allow the asperities to break through any developed contaminants as well as reduce electrical contact resistance by appropriately applying force along the conducting asperities. This novel concept was simulated to verify that the contact resistance of an outer rim maximum load and current density asperity contact interface design can be significantly lower than a similarly finished Hertzian style contact interface. Based on simulation, the final results revealed that the greatest contact resistance reduction (up to a factor of 2) occurred for a mated Sn finished surface.[88]

5. Failure modes and reliability

There are a number of potential applications for MEMS switches and relays if the problems identified can be resolved. The target is to actuate billions of switching cycles with low current loading. Typically, designs are for a supply voltage of 4–5 Volts; which is below the minimum voltage required for arcing and a switching current below the minimum arcing current. If the supply current exceeds this minimum, there will be a discharge process which will degrade the switching performance. The lower limits of arcing are not clearly defined and will be influenced by any inductance and capacitance in the circuit. The occurrence of arcing will depend on the contact materials as well as the distance between the upper and lower contacts. At the lower limits of supplied current and voltage, arcing is predicted with a probability function. For switching applications, it is desirable to have no arcing. It was suggested by Jemaa and Hasegawa that for Au contacts the lower limit for no arcing is 80 mA, however, these experiments were conducted at a voltage above the minimum arcing voltage.[89–91] In the context of RF switching, an investigation of the basic switching phenomena was provided by Johler and Miki *et al* in these examples, arcing was present between the contacts.[92,93]

Contact bounce, occurring at switch closure, can greatly impact the performance and lifetime of micro-switch electrical contacts. This phenomenon has been widely studied in macro, as well as micro-devices.[13,94–102] In MEMS, switch designers have focused on suppressing or 'engineering away' contact bounce using mechanical switch designs or novel actuation signals that aim for near zero impact velocity of the electric contacts.[96–102] Peschot *et al* however, performed experiments to better explain contact bounce at the nanometer scale.[103] Using an AFM and a nano-indenter, the researchers controlled micro-contact make and break operations at low values of electrode velocity (few tens of nm s^{-1}). They discovered that the electrostatic force overcame the mechanical restoring force of the mobile contact near 10 nm. The team analytically ruled out the Casimir force by examining the effective distance for which the quantum electrodynamic force would have effect. It was found that the Casimir force was only dominant in the last few nanometers. The explanation for contact bounce was given as the product of competition between the restoring force of the contact beam and the adhesion force. The adhesion force was considered as contact interactions such as capillary, chemical, and van der Waals forces.[104] As the contact is made and the voltage between contacts is near zero the competition begins between adhesion force and restoring force. Upon opening of the contact, a potential difference is created and is the electrostatic force; which influences the contact to be made again. The final result revealed that for the given mechanical design of the beam, the velocity of the contact beam has to be higher than 1 μm s^{-1} in order to avoid bouncing due to the electrostatic force.

'Cold' switching is generally known to be actuating the switch repeatedly without applying RF or dc power during actuations, leading to micro-switch failures such as mechanical structural fatigue, memory effect, contact stiction, frictional polymer formation, thermal-mechanical damage when closed, etc.[6,13] Simply put, 'cold' switching is powering the circuit off, then actuating the switch off then on, then powering the circuit back on. To model 'cold' switching, the circuit elements would not contain stored energy at the time the switch closes and all energy would dissipate between actuations. This limits the types of failures experienced by micro-switches and extends reliability. 'Hot' switching is considered to be actuating the switch repeatedly while applying either RF or dc power during actuations.[6] Zavracky *et al* reported over 2×10^9 cycles as the lifetime for sputtered Au contacts that were packaged in nitrogen;[105] a considerable difference when compared to the 5×108 cycles Zavracky reported for 'hot-switched' contacts.[105] Majumder *et al* reports greater than 10^7 'hot-switched' cycles and approximately 10^{11} 'cold-switched' cycles for micro-switches with a 'platinum group' contact metal.[106] Newman *et al* also performed independent lifetime measurements on high-reliability, commercial contact switches and reported average cold switched lifetimes of 430×10^9 cycles.[107,108] Czaplewksi *et al* reported

10^{10} switching cycles using RF MEMS switches fabricated with RuO_2—Au contact metals.[52] In comparison, 'hot-switched' at 4 V, 20 mA, Au coated MWCNT contacts exhibited 7×10^7 cycles in initial studies.[109]

Toler and Coutu characterized the impact on reliability of external resistive, inductive, and capacitive loads for micro-switches.[110] Certain configurations of loads were determined to enhance micro-switch reliability. Specifically, that an external resistive load in series acts as a current limiter for both 'hot' and 'cold' switching conditions and reduces the probability of an electrical failure mode thereby enhancing the reliability of the micro-switch. In addition, there is a possibility of increasing the reliability of the switch by using a higher resistance contact metals with a matching external resistive load. The current limiting effect would restrict temperature and increased hardness of the higher resistance contact metal would most likely extend the reliability of the micro-switch further than a low resistance contact metal. Alternatively, it was found that certain configurations of resistive, inductive, and capacitive loads promote early failure via increased material transfer and current density. An external capacitive load in parallel was determined to be detrimental to micro-switch reliability under 'hot' switching conditions since it compounded the current during discharge and raised the probability for increased current density, temperature, and material transfer. For 'cold' switching conditions, the discharge of the capacitor essentially continues to provide current through the contact after the signal has stopped transmitting and before the switch opens; effectively turning a 'cold' switching condition into a 'hot' switching condition and reducing reliability with the increased probability of electrical failure. Lastly, the external inductive load for dc conditions reduced susceptibility of failure via increased current density and temperature by limiting the current at the moment of initial contact in 'hot' switching conditions. 'Cold' switching conditions for external inductive loads have negligible effect to contact resistance and micro-switch reliability.

As mentioned earlier, stiction or adhesion is a failure mode which is commonly caused by capillary, electrostatic, chemical, and van der Waals forces.[104] The surface of contacts in air can become hydrophilic due to oxidation and formation of a liquid meniscus by water vapor resulting in stiction.[83] Many researchers have proposed reducing the surface adhesion force by novel switch design, contact materials, and sealing the micro-contacts in inert gases.[3,83,111–114] Adhesion can be described by Hertz, JKR, or DMT theories.[115] Hertz theory, mentioned in the contact resistance modeling section, is traditionally used for modeling elastic adhesion between non-deformable surfaces.[115] For deformable surfaces, JKR or DMT theory is utilized. JKR theory takes into account the surface energy of the contacting interfaces. Comparatively, DMT theory emphasizes the cohesive forces at the contact periphery.[115] The JKR model is valid for 'soft' elastic materials with higher surface energy while the DMT model is applicable for 'hard' stiff solids with low surface energy.[115]

A multiscaled approach was developed by Wu *et al* in order to predict stiction due to Van der Waals forces.[116] For micro-scale calculations, the unloading adhesive contact-distance curves of two interacting rough surfaces were established from a combination of an asperity model and the Maugis transition theory.[116] The computed unloading distance curves were dependent on the material and surface properties such as roughness discussed earlier in this chapter.[116] The model was then integrated into a macro-model for the ease of finite element analysis.[116] The parameters for the FEM in terms of surface topography and micro-geometry were evaluated from theoretical models, surface energy measurements, or AFM measurements.[116] The key advantage of the model is its ability to account for a wide variety of micro-scale parameters such as surface topography, surface cleanliness, etc. while still enabling complete modeling of the larger MEMS structure using FEM.[116] The disadvantage of this approach is the absence of the effect of capillary forces.[116]

Fretting is a form of structural fatigue which is defined as accelerated surface damage occurring at the interface of contacting materials subjected to small oscillatory movements.[7] Braunovic states that the lack of published information of failures due to fretting is because fretting is a 'time-related process causing an appreciable effect

only after a long period of time as a result of the accumulation of wear debris and oxides in the contact zone'.[7] However, contact force has significant influence on the contact resistance in fretting conditions. As the force applied on the contact is increased, the contact resistance declines until there is a significant amount of wear debris and oxide to form an insulating layer. As the insulating layer develops, the resistance increases despite larger applications of force. Fretting is a rate dependent phenomenon and the frequency of oscillations will affect the contact resistance.

Another 'cold' switch mechanical failure cause is pitting. Pitting and hardening occur when two metals make contact repeatedly at the same location.[1] The repeated actuations create cavities at the surface and are confined to a point or small area.[7] The areas are described as being irregularly shaped and are filled with corrosion products over time.[7] The buildup of corrosion products in conjunction with pitting reduces the area available for current flow and will induce high temperatures at those areas while the switch is closed. The result will be a localized high temperature failure mode as seen in 'hot' switching conditions.

According to Kim, the lifetime of a switch is more restricted by 'hot'-switching than by 'cold'-switching because most of the signals that are transmitted through the switch have high power loads.[6] Electrical failure mechanisms, like temperature, current density, and material transfer are all factors in reliability under 'hot' switching.[1] With an emphasis on no arcing, the transfer of material between electrical contacts in MEMS devices below the minimum arcing voltage is known as 'fine transfer'.[116] A major consideration in 'hot' switching is a large temperature rise which occurs in the contact region due to the small contact area on the a-spots.[1] With a small contact region comes a large contact resistance, which in the case of 'hot'-switching will result in large heat dissipation in that area at the time the switch closes. Increased temperature at these localized points may soften the contact metal and lead to bridge transfer. A problem with bridge transfer is that the internal stresses cause the contact metal to shrink and crack.[7] Oxidation then leads to a reduced number of electrical conducting paths thereby leading to overheating and ultimately failure.[7]

An increase in current density raises the temperature for the contact areas on the cathode and anode. Concerning the topology of the contact surface, which has asperities, a higher current density will cause high temperature spots at asperities. The relationship between the temperature in the contact and voltage drop across the contact is described as:

$$V_c^2 = 4L(T_c^2 - T_o^2) \tag{25}$$

$$V_c^2 = 4L(T_c^2 - T_o^2)$$

where V_c is the voltage drop across the contact, L is the Lorenz constant (approximately 2.4×10^{-8} V °K^{-1} for most metals), T_c is the temperature in the contact, and T_o is the bulk temperature.[16]

It is important to note that the relationship between voltage and temperature above does not consider the size effects of the asperities in contact.[117] Examining (25), an increase in current would result in an increase in temperature due to I^2Rloss. The resistance is expected to increase because of the metal's positive temperature coefficient of resistance, α. The equation for resistance R_c, at the new temperature T_c is then:

$$R_c(T_C) = R_{co}\left[1 + \tfrac{2}{3}\alpha(T_c - T_o)\right] \tag{26}$$

$$R_c(T_C) = R_{co}\left[1 + \frac{2}{3}\alpha(T_c - T_o)\right]$$

but (26) only holds true until a temperature is reached that softening of the metal begins to occur.[16] When the contact metals soften the asperities collapse, increasing their areas to facilitate cooling. The collapsing of asperities increases the effective contact area and results in a decrease of the contact resistance. The plastic deformation of the asperities during the contact formation proceeds more rapidly when the softening temperature is reached.[74] This is seen by contact resistance as a function of area:

$$R_c = \frac{\rho}{2}\sqrt{\frac{1}{2R\alpha}} \qquad\qquad (27)$$

$$R_c = \frac{\rho}{2}\sqrt{\frac{1}{2R\alpha}}$$

and R is asperity peak radius of curvature and α is asperity vertical deformation.[19] Immediately following initial asperity deformation, contact asperities are susceptible to creep under compressive strain.[41] Creep deformation has been reported by Gregori *et al* as well as Budakian *et al* at micro-Newton level contact forces and low current levels.[118,119] With creep, the contact material deforms and reduces the contact pressure, resulting in increased contact resistance.[7]

The softening of the metal at the asperities of the contact reduces the strain hardening of the a-spots and could accelerate the aging of the contact by the activation of thermal failure mechanisms such as bridge transfer.[55] High temperature for the small volumes of material changes the softness of the contact material and promotes bridge transfer. Holm noted that material transfer of very small volumes of material was known originally as fine transfer and said the phenomena is usually called bridge transfer. Bridge transfer is a form of material transfer which reduces the effective area of the asperities and increases the contact resistance.[13] Also, increased temperature decreases the mobility of electrons in a metal, resulting in increased resistivity. If the choice of contact materials is not appropriate, the materials may not be able to conduct away the resistive heat generated by currents passing through surface asperities, the large local temperature increases and will further the probability of bridge transfer.[85,120] Changes to the surface topology are detrimental to contact resistance. When the contact opens, a newly ruptured bridge can provide better conditions for field emission when the electrodes are in close proximity and a voltage exists across them. Temperature is an important consideration for contact design. Increased contact temperatures can sometimes activate diffusion and oxidation processes that are driven by elevated temperatures, which ultimately reduces surface conductivity and contact resistance will increase.[121,122]

Dickrell and Dugger simulated a Au-Pt micro-contact using a nanoindentor in order to test and examine the performance of Au-Pt contacts.[23] The experiment showed that the contact experienced a dramatic increase in contact resistance, by orders of magnitude, when hot-switched in both ambient and inert nitrogen environments.[23] The results indicated that arc formation at the time of opening or closing was the cause of increased resistance.[23] Arcing resulted in a decomposition of the surface contaminants and the creation of an insulating surface layer.[23]

Considering dc, electromigration is another form of material transfer which causes micro-switch failure.[7] Electromigration is defined as 'the forced motion of metal ions under the influence of an electric field'.[7] Atomic flux (J) is given by:

$$J = \frac{D}{kT} J\rho eZ^* \tag{28}$$

$$D = D_o e^{-\frac{Q}{kT}} \tag{29}$$

where D is the diffusion coefficient, J is the current density, ρ is the electrical resistivity and eZ^* is the effective charge, k is the Boltzmann constant, T is the absolute temperature, D_o and Q are the diffusivity constant and activation energy for diffusion, respectively.[7] As shown by (28), atomic flux is directly proportional to current density. Voids form as a result of electromigration and ultimately cause device failure.[8] Braunovic states that an increase in current density in the a-spots can be substantial and create the right conditions for electromigration to occur.[7]

Distinct from electromigration, field emission is also responsible for material transfer phenomena.[123] Field emission is the transfer or emission of electrons induced by an electrostatic field. Literature in this area is limited, however, Poulain et al conducted an investigation into the phenomena using a modified atomic force microscope.[123] The results showed a current increase when the contact gap became smaller than a few tens of nanometers.[123] At that range, the team deduced that the emission of electrons from the cathode followed the Fowler–Nordheim theory and led to damage on the opposite contact member.[123] The damage to the opposite contact consisted of evaporated anode material caused by impact heating (electrons leaving the anode heated the material and caused evaporation of anode contact material to the cathode interface).[123] The reported transfer of material due to field emission occurred with an open-circuit voltage across the two contact members of 5 V and a test current limited to 1 mA when the contact was closed. These results corroborate those of Yang et al who demonstrated micro-contact degradation under various hot/cold switching conditions.[124] Additionally, Yang et al hypothesized that the observed field-induced material transfer was due to the contact's open-circuit voltage being greater than the field evaporation threshold of the electric contact material.[124]

Additionally, Hennessy et al investigated Ru–Ru contacts, using a custom built testing apparatus, with approximately 400 µN of applied contact force under dc 'hot-switched' conditions.[125] In this configuration, they observed and compared both leading and trailing edge hot switching events with trailing edge phenomena leading to higher contact adhesion. In addition, they observed polarity dependent material transfer during short duration current spike events associated with bias voltages greater than 1.5 V.[125] Although, these results do not confirm previous material transfer phenomena they clearly show multiple mechanisms being active during each 'hot' switching cycle.[125]

For complete integration with CMOS processes, micro-switches need to withstand temperatures of about 400 °C without a change in performance.[126] At high temperatures, cantilever beams normally begin to deflect due to intrinsic stresses in the layered materials making up the beam. Klein et al designed an electrostatically actuated micro-switch based on a tungsten-titanium alloy to reduce the possibility of failure due to temperature and stiction.[126] Klein et al chose tungsten for its high melting point of 3370 °C, which is a good indicator of stability for temperatures a tenth of the melting point value.[126] The tungsten–titanium alloy switches were evaluated to temperatures up to 500 °C and the results indicate that the design is stable with beam deflections of only 8%.[126]

Insertion loss was reported to be slightly higher than compared to more conductive switches but isolation was comparable.[126]

No discussion of failure modes is complete without a discussion of frictional polymers. Metals most susceptible to the development of frictional polymers are the 'platinum group' metals and any other 'catalytically active metal'.[7] Holm pointed out that thin films, like oxides, develop over time on the contact surface and act as insulators, greatly increasing contact resistance.[13] The same is true for micro-switches. Though much smaller than the contacts studied by Holm, the effects of the films which develop on micro-contacts are orders of magnitude greater than those that develop on macro scale contacts. Contaminant films on micro-contacts can render the contact useless and disabled. A particularly damaging film is the development of a frictional polyme.[7] Frictional polymers are organic films, sometimes referred to as deposits, that develop on commonly used contact materials when low levels of organic vapors or compounds are introduced into the operating environment of the contact.[7] Czaplewksi *et al.* lifecycle tested RF MEMS switches fabricated with Au-Ir and Au-Pt contacts and verified carbon-based contaminant films building up on the electric contacts.[127] In this study the authors used SEM inspection and Auger electron spectroscopy (AES) to verify the presence of carbon contamination.[127] Crossland and Murphy, however, were able to show that the addition of a non-catalytically active metal, like silver, can significantly reduce the effects of frictional polymerization.[128] Though silver is not considered suitable for MEMS due to tarnishing, their experiment showed that silver must make up 36% or more of the contact materials in order to witness a significant reduction.[128] In comparison, Czaplewksi *et al* used catalytically less active contact materials (RuO_2-Au) in RF MEMS micro-switches resulting in longer lifetimes.[52] This result was corroborated by de Boer *et al* who studied RuO_2-Au contacts in ultra-clean environments, cycled using polysilicon test structures.[129] After 3×10^9 cycles, AES results indicated no noticeable difference in carbon concentration in either the contact or non-contacting areas, thus implying that carbon build-up or 'frictional polymer' was not a limiting factor in micro-switch reliability when using contact materials with lowered catalytic activity.[129]

6. Conclusion

This review provides insight into the properties and concepts necessary for designing micro-electrical contacts for dc and RF MEMS switches. The basic theories behind the aspects of design, contact resistance modeling, contact materials, and failure modes are discussed and explored. A survey of the challenges for these areas in ohmic contacts is provided. Complete models of contact resistance for various electron transport modes and deformation models are shown. The decision for contact materials is investigated by examining the impact of material properties on the characterization of the contact.

Acknowledgments

References

[1] Rebeiz G 2004 *RF MEMS, Theory, Design, and Technology* (Hoboken, NJ: Wiley)

[2] Van Caekenberghe K 2009 RF MEMS on the radar *IEEE Microw. Mag.* **10** 99–116

[3] Yang Z, Lichtenwalner D, Morris A, Krim J and Kingon A 2009 Comparison of Au and Au-Ni alloys as contact materials for MEMS switches *IEEE J. Microelectromech. Syst.* **18** 287–95

[4] Dennard R, Cai J and Kumar A 2007 A perspective on today's scaling challenges and possible future directions *Solid State Electron.* **51** 518–25

[5] Kaynak M, Ehwald K, Sholz R, Korndorfer F, Wipf C, Sun Y, Tillack B, Zihir S and Gurbuz Y 2010 *Characterization of an embedded RF-MEMS switch SiRF' 10: Topical Meeting on Silicon Monolithic Integrated Circuits in RF Systems (SiRF)* (New Orleans, LA,) pp 144–7

[6] Kim J, Lee S, Baek C, Kwon Y and Kim Y 2008 Cold and hot switching lifetime characterizations of ohmic contact RF MEMS switches *IEICE Electron. Express* **5** 418–23

[7] Braunovic M, Konchits V and Myshkin N *2007 Electrical Contacts—Fundamentals Applications, and Technology* (New York: CRC Press)

[8] Lee K I 2011 Bang, *Principles of Microelectromechanical Systems* (Hoboken, NJ: Wiley)

[9] Kaajakari V 2009 *Practical MEMS* (Las Vegas, Nevada: Small Gear publishing)

[10] Kovacs G 1998 *Micromachined Transducers Sourcebook* (New York: McGraw-Hill)

[11] Comtois J, Michalicek M and Barron C 1997 Fabricating micro-instruments in surface-micromachined polycrystalline silicon *Proc. 43rd Int. Instrumentation Symp.* pp 169–78

[12] Lucyszyn S 2004 Review of radio frequency microelectromechanical systems technology *IEE Proc.* **151** 93–103

[13] Holm R 1967 *Electric Contacts: Theory and Applications* 4th edn (Berlin: Springer)

[14] Coutu R A Jr, McBride J W and Starman L A 2009 Improved micro-contact resistance model that considers material deformation, electron transport and thin film characteristics *Proc. 55th IEEE Holm Conf. on Electrical Contacts* (Vancouver, BC, Canada,) pp 296–9

[15] Majumder S, McGruer N, Adams G, Zavracky P, Morrison R and Krim J 2001 Study of contacts in an electrostatically actuated microswitch *Sensors Actuators* **93** 19–26

[16] Pitney K 1973 *Ney Contact Manual* (Bloomfield: J M Ney Company)

[17] Chang W R 1997 An elastic-plastic model for a rough surface with an ion-plated soft metallic coating *J. Wear* **212** 229–37

[18] Abbot E and Firestone F 1933 Specifying surface quantity—a method based on the accurate measurement and comparison *ASME Mech. Eng.* **55** 569

[19] Coutu R A Jr, Reid J, Cortez R, Strawser R and Kladitis P 2006 Microswitches with Sputtered Au, AuPd, Au-on-AuPt, and AuPtCu alloy electrical contacts *IEEE Trans. Compon. Packag. Technol.* **29** 341–9

[20] Wexler G 1966 The size effect and the non-local Boltzmann transport equation in orifice and disk geometry *Proc. Phys. Soc.* **89** 927–41

[21] Mikrajuddin A, Shi F and Okyuama K 1999 Size-dependent electrical constriction resistance for contacts of arbitrary size: from Sharvin to Holm limits *Proc. Mater. Sci. Sem.* **2** 321–7

[22] Karmalkar S, Mohan P and Kumar B 2005 A unified compact model of electrical and thermal 3-d spreading resistance between eccentric rectangular and circular contacts *IEEE Electron Device Lett.* **26** 909–12

[23] Dickrell D and Dugger M 2007 Electrical contact resistance degradation of a hot-switched simulated metal MEMS contact *IEEE Trans. Compon. Packag. Technol.* **30** 75–80

[24] Patton S, Eapen K and Zabinski J 2001 Effects of adsorbed water and sample aging in are on uN level adhesion force between Si(1 0 0) and silicon nitride *Tribol. Int.* **34** 481–91

[25] Lumbantobing A, Kogut L and Komvopoulos K 2004 Electrical contact resistance as a diagnostic tool for MEMS contact interfaces *J. Microelectromech. Syst.* **13** 977–87

[26] Timsit R 2010 Constriction resistance of thin film contacts *IEEE Trans. Compon. Packag. Technol.* **33** 636–42

[27] Norberg G, Dejanovic S and HesselBom H 2006 Contact resistance of thin metal film contacts *IEEE Trans. Compon. Packag. Technol.* **29** 371–8

[28] Timsit R 2006 Electrical conduction through small contact spots *IEEE Trans. Compon. Packag. Technol.* **29** 727–34

[29] Agrait N, Yeyati A and Ruitenbeek J 2003 Quantum properties of atom-sized conductors *Phys. Reports* **377** 81–279

[30] Sawada S, Tsukiji S, Tamai T and Hattori Y 2012 Current density analysis of thin film effect in contact area on LED wafer Proc. *58th IEEE Holm Conf. on Electrical Contacts* pp 242–7

[31] Jackson R, Crandall E and Bozak M J 2012 An analysis of scale dependent and quantum effects on electrical contact resistance between rough surfaces *Proc. 58th IEEE Holm Conf. on Electrical Contacts* pp 1–8

[32] Poulain C, Jourdan G, Peschot A and Mandrillon V 2010 Contact conductance quantization in a MEMS switch *Proc. 56th IEEE Holm Conf. on Electrical Contacts* pp 1–7

[33] Pennec F, Peyrou D, Leray D, Pons P, Plana R and Courtade F 2012 Impact of the surface roughness description on the electrical contact resistance of ohmic *IEEE Trans. Compon. Packag. Manuf. Technol*. **2** 85–94

[34] McCool J 1986 Comparison of models for the contact of rough surfaces *Wear* **107** 37–60

[35] Majumdar A and Bhushan B 1990 Role of fractal geometry in roughness characterization and contact mechanics of surfaces *ASME J. Tribol*. **112** 205–16

[36] Majumdar A and Tien C 1990 Fractal characterization and simulation of rough surfaces *Wear* **136** 313–27

[37] Kogut L and Jackson R 2005 A comparison of contact modeling utilizing statistical and fractal approaches *ASME J. Tribol*. **128** 213–7

[38] Kogut L and Etsion I 2003 A finite element based elastic-plastic model for the contact of rough surfaces *Tribol. Trans*. **46** 383–90

[39] Greenwood J and Williamson J 1966 Contact of nominally flat surfaces Proc. R. Soc. *A* **295** 300–19

[40] Greenwood J 1984 A unified theory of surface roughness *Proc. R. Soc. A* **393** 133–57

[41] Rezvanian O, Zikry M, Brown C and Krim J 2007 Surface roughness, asperity contact and gold RF MEMS switch behavior *J. Micromech. Microeng*. **17** 2006–15

[42] Borri-Brunetto M, Chiaia B and Ciavarella M 2001 Incipient sliding of rough surfaces in contact: a multiscale numerical analysis *Comput. Methods Appl. Mech. Eng.* **190** 6053–73

[43] Komvopoulos K and Ye N 2001 Three-dimensional contact analysis of elastic-plastic layered media with fractal surface topographies *ASME J. Tribol*. **123** 632–40

[44] Persson B, Bucher F and Chiaia B 2002 Elastic contact between randomly rough surfaces: comparison of theory with numerical results *Phys. Rev. B* **65** 184106

[45] Persson B 2001 Elastoplastic contact between randomly rough surfaces *Phys. Rev. Lett.* **87** 116101

[46] Jackson R and Streator J 2006 A multi-scale model for contact between rough surfaces *Wear* **261** 1337–47

[47] Wilson W, Angadi S and Jackson R 2008 Electrical contact resistance considering multi-scale roughness *Proc. 54th IEEE Holm Conf. on Electrical Contacts* pp 190–7

[48] Jackson R 2011 A model for the adhesion of multiscale rough surfaces in *MEMS SSST' 11: IEEE 43rd Southeastern Symp. on System Theory (SSST)* pp 257–62

[49] Jackson R and Kogut L 2007 Electrical contact resistance theory for anisotropic conductive films considering electron tunneling and particle flattening *IEEE Trans. Compon. Packag. Technol*. **30** 59–66

[50] Coutu R A Jr, Kladiti S P, Leedy K and Crane R 2004 Selecting metal allow electric contact materials for MEMS switches *J. Micromech. Microeng*. **14** 1157–64

[51] Broue A, Dhennin J, Charvet P, Pons P, Jemaa N, Heeb P, Coccetti F and Plana R 2010 Multiphysical characterization of micro-contact materials for MEMS switches *Proc. 56th IEEE Holm Conf. on Electrical Contacts* pp 363–72

[52] Czaplewski D A, Nordquist C D, Patrizi G A, Kraus G M and Cowan W D 2013 RF MEMS switches with RuO2-Au contacts cycles to 10 billion cycles *J. Microelectromech. Syst.* **22** 655–61

[53] ASM 1990 *Metals Handbook* vol 2 (Materials Park, OH: American Society for Metals Int.)

[54] Arrazat B, Duvivier P, Mandrillon V and Inal K 2011 Discrete analysis of gold surface apserities deformation under spherical nano-indentation towards electrical contact resistance calculation *Proc. IEEE 57th Holm Conf. on Electrical Contacts* pp 167–74

[55] Broue A, Dhennin J, Courtade F, Dieppedale C, Pons P, Lafontan X and Plana R 2010 Characterization of Au/Au, Au/Ru and Ru/Ru ohmic contacts in MEMS switches improved by a novel methodology *J. Micro/Nanolithogr., MEMS, and MOEMS* **9** 041102

[56] McGreuer N, Adams G, Chen L, Guo Z and Du Y 2009 Mechanical, thermal, and material influences on ohmic-contact-type MEMS switch operation MEMS' 06: *Proc. 19th IEEE Int. Conf. on Micro Electro Mechanical Systems (Istanbul, Turkey,)* pp 230–3

[57] Kwon H, Choi D, Park J, Lee H, Kim Y, Nam H, Joo Y and Bu J 2007 Contact materials and reliability for high power RF-MEMS switches MEMS' *07: IEEE 20th Int. Conf. on Micro Electro Mechanical Systems (Kobe,)* pp 231–4

[58] Yaglioglu O, Hart A, Martens R and Slocum A 2006 Method of characterizing electrical contact properties of carbon nanotube coated surfaces *Rev. Sci. Instrum.* **77** 095105

[59] Thostenson E, Ren Z and Chou T 2001 Advances in the science and technology of carbon nanotubes and their composites: a review *Compos. Sci. Technol.* **61** 1899–912

[60] Yunus E, McBride J and Spearing S 2009 The relationship between contact resistance and contact force on au-coated carbon nanotube surfaces under low force conditions *IEEE Trans. Compon. Packag. Technol.* **32** 650–7

[61] Choi J, Lee J, Eun Y, Kim M and Kim J 2011 Microswitch with self-assembled carbon nanotube arrays for high current density and reliable contact *MEMS' 11: IEEE 24th Int. Conf. on Micro Electro Mechanical Systems (MEMS) (Cancun,)* pp 87–90

[62] Chai Y, Hazeghi A, Takei K, Chen H, Chan P, Javey A and Wong H 2012 Low-resistance electrical contact to carbon nanotubes with graphitic interfacial layer *IEEE Trans. Electron Devices* **59** 12–19

[63] Gambino J and Colgan E 1998 Silicides and ohmic contacts *Mater. Chem. Phys.* **52** 99–146

[64] Kim W, Javey A, Tu R, Cao J, Wang Q and Dai H 2005 Electrical contacts to carbon nanotubes down to 1nm in diameter *Appl. Phys. Lett.* **87** 101–73

[65] Chai Y, Hazegh I A, Takei K, Chen Y, Chan P, Javey A and Wong H 2010 Graphitic interfacial layer to carbon nanotube for low electrical contact resistance *IEDM Technol. Digest* **9** 210–3

[66] Chen Q, Wang S and Peng L 2006 Establishing ohmic contacts for in situ current–voltage characteristic measurements on a carbon nanotube inside the scanning electron microscope *Nanotechnology* **17** 1087–98

[67] Rykaczewski K, Henry M, Kim S, Fedorov A, Kulkarni D, Singamaneni S and Tsukruk V 2010 The effect of geometry and material properties of a carbon joint produced by electron beam induced deposition on the electrical resistance of a multiwalled carbon nanotube-to-metal contact interface *Nanotechnology* **21** 1–12

[68] Ke F, Miao J and Oberhammer J 2008 A ruthenium-based multimetal-contact RF MEMS switch with a corrugated diaphragm *J. Microelectromech. Syst.* **17** 1447–59

[69] Lee H, Coutu R A Jr, Mall S and Leedy K 2006 Characterization of metal and metal alloy films as contact materials for MEMS switches *J. Micromech. Microeng.* **16** 557–63

[70] Cha P, Srolovitz D and Vanderlick T 2004 Molecular dynamics simulation of single asperity contact *Acta Mater.* **52** 3983–96

[71] Song J and Srolovitz D 2007 Atomistic simulation of multi-cycle asperity contact *Acta Mater.* **55** 14

[72] Kuipers L and Frenken J 1993 Jump to contact, neck formation, and surface melting in the scanning tunneling microscope *Phys. Rev. Lett.* **70** 3907–10

[73] Patton S and Zabinski J 2005 Fundamental studies of Au contacts in MEMS RF switches *Tribol. Lett.* **18** 215–30

[74] Fortini A, Mendelev M, Buldyrev S and Srolovitz D 2008 Asperity contacts at the nanoscale: comparison of Ru and Au *J. Appl. Phys.* **104** 074320

[75] Frenkel D and Smit B 2002 Understanding Molecular Simulation (*Computational Science Series* vol 1) 2nd edn (New York: Academic)

[76] Sorensen M, Brandbyge M and Jacobsen K 1998 Mechanical deformation of atomic-scale metallic contacts: Structure and mechanisms *Phys. Rev*. B **57** 3283–94

[77] Du Y, Chen L, McGruer N, Adams G and Etsion I 2007 A finite element model of loading and unloading of an asperity contact with adhesion and plasticity *J. Colloid Interface Sci*. **312** 522–8

[78] Chen Y, Nathanael R, Jeon J, Yaung J, Hutin L and Liu T 2012 Characterization of contact resistance stability in MEM relays with tungsten electrodes *J. Microelectromech. Syst.* **99** 1–3

[79] Kam H, Pott V, Nathanael R, Jeon J, Alon E and Liu T 2009 Design and reliability of a micro-relay technology for zero-standby-power digital logic applications *IEDM Tech. Digest* **33** 809–11

[80] Deal B and Grove A 1965 General relationship for the thermal oxidation of silicon *J. Appl. Phys*. **36** 3770–8

[81] Spencer M et al 2011 Demonstration of integrated micro-electro-mechanical relay circuits for VLSI applications *IEEE J. Solid-State Circuits* **46** 308–20

[82] Chandler R, Park W, Li H, Yama G, Partridge A, Lutz M and Kenny T 2003 Single wafer encapsulation of MEMS devices *IEEE Trans. Adv. Packag*. **26** 227–32

[83] Yamashita T, Itoh T and Suga T 2011 Investigation of anti-stiction coating for ohmic contact MEMS switches with thiophenol and 2-naphtalenethiol self-assembled monolayer *Sensors Actuators* A **172** 455–61

[84] Tang W, Xu K, Wang P and Li X 2003 Surface roughness and resistivity of Au film on Si-(1 1 1) substrate *Microelectron. Eng*.**66** 445–50

[85] Hyman D and Mehregany M 1999 Contact physics of gold microcontacts for MEMS switches *IEEE Trans. Compon. Packag. Technol*. **22** 357–564

[86] Kataoka K, Itoh T and Suga T 2003 Characterization of fritting phenomena on Al electrode for low contact force probe card *IEEE Trans. Compon. Packag. Technol.* **26** 382–7

[87] Baek S and Fearing R 2008 Reducing contact resistance using compliant nickel nanowire arrays *IEEE Trans. Compon. Packag. Technol*. **31** 859–68

[88] Myers M, Leidner M, Schmidt H, Sachs S and Baeumer A 2012 Contact resistance reduction by matching current and mechanical load carrying asperity junctions *Proc. 58th IEEE Holm Conf. on Electrical Contacts* pp 248–51

[89] Jemaa N 2001 Short arc duration laws and distributions at low current(<1A) and voltage (14–42Vdc) *IEEE Trans. Compon. Packag. Technol*. **24** 358–63

[90] Jemaa N 2002 Contacts conduction and switching in dc levels *Proc. 48th IEEE Holm Conf. on Electrical Contacts* pp 1–15

[91] Hasegawa M and Kamada Y 2005 An experimental study on re-interpretation of minimum arc current of electrical contacts *IEICE Trans. Electron*. **8** 1616–9

[92] Johler W 2007 Basic investigations for switching of RF signals *Proc. 53rd IEEE Holm Conf. on Electrical Contacts* pp 229–38

[93] Miki N and Sawa K 2010 Arc extinction characteristics in power supply frequencies from 50 Hz to 1 Mhz *Eur. Phys. J—Appl. Phys*. **50** 12903

[94] McBride J W 1989 Electrical contact bounce in medium-duty contacts *IEEE Trans. Compon. Hybrids Manuf. Technol.* **12** 82–90

[95] McBride J W and Sharkh S M 1992 Electrical contact phenomena during impact *IEEE Trans. Compon. Hybrids Manuf. Technol.* **15** 184–92

[96] McCarthy B, Adams G, McGruer N and Potter D 2002 A dynamic model, including contact bounce, of an electrostatically actuated microswitch *J. Microelectromech. Syst.* **11** 276–83

[97] Czaplewski D A, Dyck C W, Sumali H, Massad J E, Kuppers J D, Reines I and Cowan W D 2006 A soft-landing waveform for actuation of a single-pole single-throw Ohmic RF MEMS switch *J. Microelectromech. Syst.* **15** 1586–94

[98] Sumali H, Massad J E, Czaplewski D A and Dyck C W 2007 Waveform design for pulse-and-hold electrostatic actuation in MEMS *Sensors Actuators* A **134** 213–20

[99] Guo Z J, McGruer N E and Adams G G 2007 Modeling, simulation and measurement of the dynamic performance of an ohmic contact, electrostatically actuated RF MEMS switch *J. Micromech. Microeng*. **17** 1899–909

[100] Blecke J C, Epp D S, Sumali H and Parker G G 2009 A simple learning control to eliminate RF MEMS switch bounce *J. Microelectromech. Syst*. **18** 458–65

[101] Tazzoli A, Barbato M, Mattiuzzo F, Ritrovato V and Meneghesso 2010 Study of the actuation speed, bounces occurences, and contact reliability of ohmic *RF MEMS switches Microelectron.* Reliab. **50** 1604–8

[102] Spasos M and Nilavalan R 2011 On the investation of a reliable actuation control method for ohmic *RF MEMS switches Microelectron. J.* **42** 1239–51

[103] Peschot A, Poulain C, Bonifaci N and Lesaint O 2012 Contact bounce phenomena in a MEM switch *Proc. 58th IEEE Holm Conf. on Electrical Contacts* pp 49–55

[104] Maboudian R and Howe R 1997 Critical review: adhesion in surface micromechanical structures *J. Vac. Sci. Technol.* B **15** 1–20

[105] Zavracky P, Majumber S and McGruer N 1997 Micromechanical switches fabricated using nickel surface micromachining *J. Microelectromech. Syst*. **6** 3–9

[106] Majumder S, Lampen J, Morrison R and Maciel J 2003 MEMS Switches *IEEE Instrum. Meas. Mag.* **6** 12–15

[107] Newman H, Ebel J, Judy D and Maciel J 2008 Lifetime measurements on a high-reliability RF-MEMS contact switch *IEEE Microw. Wirel. Compon. Lett*. **2** 100–2

[108] Maciel J, Majumder S, Morrison R and Lampen J 2004 Lifetime characteristics of ohmic MEMS switches *Proc. SPIE* **5343** 1–6

[109] McBride J W 2010 The wear processes of gold coated multi-walled carbon nanotube surfaces used as electrical contact for micro-mechanical switching *Nanosci. Nanotechnol. Lett*. **4** 357–61

[110] Toler B and Coutu R A Jr 2013 Characterizing external resistive, inductive and capacitive loads for micro-switches *MEMS and Nanotechnol*. **42** 11–18

[111] Mercado L, Kuo S, Lee T and Liu L 2004 Mechanism-based solutions to RF MEMS switch stiction problem *IEEE Trans. Compon. Packag. Technol*. **27** 560–70

[112] Peroulis D, Pacheco S, Sarabandi K and Katehi L 2003 Electromechanical considerations in developing low-voltage *RF MEMS switches IEEE Trans. Microw. Theory Technol*. **51** 259–70

[113] Park J, Shim E, Choi W, Kim Y, Kwon Y and Cho D 2009 A non-contact-type RF MEMS switch for 24-GHz radar applications *J. Microelectromech. Syst*. **18** 163–73

[114] Brown C, Morris A, Kingon A and Krim J 2008 Cryogenic performance of RF MEMS switch contats *J. Microelectromech. Syst.* **17** 1460–7

[115] Prokopovich P and Perni S 2011 Comparison of JKR and DMT based multi-asperity adhesion model: Theory and experiment *Colloids Surf. A* **383** 95–101

[116] Wu L, Noels L, Rochus V, Pustan M and Golinval J 2011 A Micro-macro approach to predict stiction due to surface contact in microelectromechanical systems *J. Microelectromech. Syst.* **20** 976–90

[117] Nikolic B and Allen P 1999 Electron transport through a circular constriction *Phys. Rev. B* **60** 3963–9

[118] Gregori G and Clarke D 2006 The interrelation between adhesion, contact creep, and roughness on the life of gold contacts in radio-frequency microswitches *J. Appl. Phys.* **100** 094904

[119] Budakian R and Putterman S 2002 Time scales for cold welding and the origins of stick-slip friction *Phys. Rev. B* **65** 235429

[120] Kruglick E and Pister K 1999 Lateral MEMS microcontact considerations *J. Micromech. Syst.* **8** 264–71

[121] Sun M, Pecht M, Natishan M and Martens R 1999 Lifetime resistance model of bare metal electrical contacts *IEEE Trans. Adv. Packag.* **22** 60–67

[122] Takano E and Mano K 1967 Theoretical lifetime of static contacts *IEEE Trans. Parts Mater. Packag.* **22** 60–67

[123] Poulain C, Peschot A, Vincent M and Bonifaci N 2011 A nano-scale investigation of material transfer phenomena at make in a MEMS switch IEEE 57th Holm Conf. on Electrical Contacts(Grenoble, France,)

[124] Yang Z, Lichtenwalner D, Morris A, Krim J and Kingon I O 2010 Contact degradation in hot/cold operation of direct contact micro-switches *J. Micromech. Microeng.* **20** 105028

[125] Hennessy R P, Basu A, Adams G G and McGruer N E 2013 Hot-switched lifetime and damage characteristics of MEMS switch contact *J. Micromech. Microeng.* **23** 1–11

[126] Klein S, Thilmont S, Ziegler V, Prechtel U, Schmid U and Seidel H 2009 High temperature stable RF MEMS switch based on tungsten-titanium *TRANSDUCERS' 09: Int. Solid-State Sensors, Actuators and Microsystems Conf.*

[127] Czaplewski D A, Nordquist C D, Dyck C W, Patrizi G A, Kraus G M and Cowan W D 2012 Lifetime limitations of ohmic, contacting RF MEMS switches with Au, Pt and Ir contact materials due to the accumulation of 'frictional polymer' on the contacts *J. Micromech. Microeng.* **22** 1–12

[128] Crossland W and Murphy P 1974 The formation of insulating organic films on palladium–silver contact alloys *IEEE Trans. Hybrids Packag.* **10** 64–69

[129] de Boer M P, Czaplewski M S, Baker M S, Wolfley S L and Ohlhausen J A 2012 Design, fabrication, performance and reliabilty of Pt- and RuO2—coated microrelays tested in ultra-high purity gas environments *J. Micromech. Microeng.* **22** 1–1